

Computational Predictive Methods for Fracture and Fatigue

J. Cordes, A.T. Chang, N. Nelson, Y. Kim
Department of Mechanical Engineering
Stevens Institute of Technology
Castle Point on the Hudson
Hoboken, New Jersey 07030

513-39
23107
p- 18

Abstract

The damage-tolerant design philosophy as used by aircraft industries enables aircraft components and aircraft structures to operate safely with minor damage, small cracks, and flaws. Maintenance and inspection procedures insure that damages developed during service remain below design values. When damage is found, repairs or design modifications are implemented and flight is resumed.

Design and redesign guidelines, such as military specifications MIL-A-83444, have successfully reduced the incidence of damage and cracks. However, fatigue cracks continue to appear in aircraft well before the design life has expired. The F16 airplane for instance, developed small cracks in the engine mount, wing support bulk heads, the fuselage upper skin, the fuel shelf joints, and along the upper wings. Some cracks were found after 600 hours of the 8000 hour design service life and design modifications were required. Tests on the F16 plane showed that the design loading conditions were close to the predicted loading conditions [1]. Improvements to analytic methods for predicting fatigue crack growth adjacent to holes, when multiple damage sites are present, and in corrosive environments would result in more cost-effective designs, fewer repairs, and fewer redesigns.

The overall objective of the research described in this paper is to develop, verify, and extend the computational efficiency of analysis procedures necessary for damage tolerant design. This paper describes an elastic/plastic fracture method and an associated fatigue analysis method for damage tolerant design. Both methods are unique in that material parameters such as fracture toughness, R-curve data, and fatigue constants are not required. The methods are implemented with a general-purpose finite element package. Several proof-of-concept examples are given. With further development, the methods could be extended for analysis of multi-site damage, creep-fatigue, and corrosion fatigue problems.

Introduction

Prediction of fracture and fatigue behavior generally requires a variety of experimentally-generated data points. For elastic/plastic fracture, resistance curves (R-curves) characterize increasing material toughness as a stable crack tip is driven through the crack tip plastic zone. Crack growth resistance curves, such as J-integral versus stable crack growth, are used to predict the onset of fracture

and the stable crack growth behavior in elastic/plastic components. JR-curves depend on thickness, component geometry in the case of center-cracked plates [2], the extent of plasticity [3], and perhaps whether the experiment is load controlled or displacement controlled [4]. Design engineers assessing residual strength must choose material parameters and resistance curves which are determined for similar geometries, thicknesses, and environmental conditions [5-7].

Efforts have been made to predict elastic/plastic fracture and stable crack growth behavior with fewer experimentally-generated data points. Shan et. al. [8] used the crack tip opening angles at crack initiation and at the onset of stable crack growth to predict stable crack growth behavior. Elangovan [9] formulated a method for generating an R-curve using two points on the R-curve. Newman et. al. [10] used a single experimentally-determined parameter, the critical crack tip opening angle, to model stable crack growth behavior in thin aluminum panels. Zhang and Gross [11] used a cohesive stress zone model to predict critical crack tip opening displacement and JR-curve behavior analytically. Fracture parameters were derived from a base fracture parameter, stress/strain diagrams, an assumed micro-damage ahead of the crack tip, and small scale yielding assumptions.

Since the early 1960's, fatigue crack growth rates have been determined using a power-law equation that requires two material constants. The linear-elastic fracture parameter ΔK was introduced by Paris and Erdogan [12] for predicting fatigue crack growth rates (1960):

$$\frac{da}{dN} = C (\Delta K)^n \quad (1)$$

where a = crack size or half-crack size
 da = increment of crack growth
 dN = # of cycles for an increment of crack growth
 C, n = material constants, determined from curve fit
 ΔK = difference in stress intensity factors evaluated at
 the maximum and minimum loading conditions

Paris' equation is limited to problems where C and n are determined for the material, where each loading cycle varies between the same maximum and minimum values, and where the size of the damage zone is small compared to the crack length. Other power-law equations have been introduced to account for the crack growth threshold load or crack initiation load [13,14], to include crack closure effects [15-20], and to include plasticity effects [21]. The crack closure methods have been particularly useful for predicting crack growth behavior under spectrum loading [22,23] and when overloads and underloads are present [24,25]. For all of the power-law equations reviewed, prior knowledge of at least two material constants is required.

The fracture and fatigue methods described in this paper rely only on material stress-strain data; additional experimental parameters and curve matching are not required. The elastic/plastic fracture method

uses a critical crack tip opening displacement curve which is generated during the analysis. The critical VR-curve is used for both the fracture and fatigue analysis method [26,27]. The methods can account for large scale yielding and large amounts of stable crack growth in thin-sheet materials as often used by the aircraft industry. Geometric dependencies are reflected in the finite element modeling. This paper provides an overview of the prediction methods, presents some validation examples, and describes the implications for future research.

Elastic/Plastic Fracture Prediction

Two basic assumptions are used in the elastic/plastic computational procedure: one concerning crack initiation and a second assumption concerning crack propagation. The finite element model incorporates a Dugdale-type cohesive zone at the crack tip and elastic/plastic material properties to model nonlinear material behavior. The cohesive zone replaces the crack-tip singularity and allows relative displacement between the crack tip grid points.

Crack initiation is assumed to occur when the crack opening displacement curve deviates by 5% from initial, linear-elastic behavior. While a mathematical proof is not offered, this assumption is consistent with ASTM specification E-399-83 [5] for brittle fracture and KIC testing. The 5% deviation point is used to determine the crack tip opening displacement at crack initiation V_1 , which occurs at the crack initiation load.

Subsequent crack growth is predicted using a critical crack tip opening displacement curve which is generated during the finite element analysis steps. For subsequent stable crack growth increments, the critical crack tip opening displacement, VR_j is found from:

$$VR_j = V_1 + V_{pw_{j-1}} \quad (2)$$

where VR_j = the critical crack tip opening displacement for crack propagation at stable crack growth Da_j
 V_1 = the crack tip opening displacement at crack initiation as calculated from the 5% offset,
 $V_{pw_{j-1}}$ = is the calculated opening displacement at the first node in the crack tip plastic wake, under applied load P_{j-1} .

Fatigue Prediction

The fatigue method uses finite element analysis, elastic/plastic fracture analysis results, and an energy approach to predict fatigue behavior. The governing equations for the fatigue analysis are:

$$N_1 = W_1/E$$

for crack initiation, and:

$$N_p = W_p/E$$

for crack propagation. Where

N_1 , N_p = the number of cycles for fatigue crack initiation or propagation

W_1 , W_p = required energy for fatigue crack initiation or propagation, determined from elastic/plastic analysis

E = energy dissipated per cycle

The available energy W is determined for each increment of crack growth by considering the available energy in the cohesive stress zone [27].

The dissipated energy 'E' depends on the applied fatigue loading condition and is an estimate of the energy consumed during each fatigue cycle. It is hypothesized that cyclic energy losses E occur when the residual compressive stress exceeds the negative yield strength of the material. The calculation for E is based on the size of the stable hysteresis loop which occurs in the stress-strain diagram. The resulting fatigue method has the following benefits: 1) Paris-type curve matching coefficients are not required, 2) the fatigue life is predicted from nonlinear analysis which includes plastic tensile strain and plastic compressive strain effects, 3) fracture and fatigue parameters are not required, 4) far-field and near-field effects of the damage are included in the analysis.

Validation of Prediction Methods

A) Elastic/Plastic Fracture Examples --

Description -- A middle-cracked panel, as described in the referenced work by Newman et. al. [10], was used to compare predicted results to experimental results and to Newman's critical crack opening angle (COA) method. The panel measured 76. mm in width, 2.3 mm in thickness, and had a crack-length to width ratio of 0.33. The material was 2024-T3 aluminum. The plate was loaded quasi-statically by an applied displacement at the boundary. The applied load, the stable crack growth increment, and the crack tip opening angle were monitored. In experiments on the middle cracked panel, the crack tip opening angle reached a constant value of 6 degrees after about 2.3 mm of stable crack growth. Newman used this 6 degree value as a single critical parameter, the crack opening angle (COA), for predicting stable crack in a middle-cracked panel.

Implementing the VR-Curve Method -- The analysis using the VR-curve method was completed using ABAQUS [28], a general purpose finite element program. Due to symmetry, one quarter of the panel was modeled using three and four node plane stress elements. An elastic/plastic material model was used for the plane stress elements. The VR-curve method was implemented as a series of load increases and model changes. At each step, the cohesive stress zone was inserted along the crack line at locations where the stress reached the yield

strength. When the critical crack tip opening displacement, as determined from equation (2) was reached, the cohesive stress at the crack tip was removed simulating crack growth.

Implementing Newman's COA Method [10] using ABAQUS -- The VR-curve results were compared to near-field results obtained using Newman's critical COA criteria. The COA method was implemented using ABAQUS, 4-node plane stress elements, and an elastic/plastic material model. The minimum element size was .3968 mm, smaller than the .48 mm element size used in the referenced paper. The critical crack opening angle was determined from the crack surface displacement two nodes behind the crack tip. Using ABAQUS, there was no difference between calculations using all plane stress elements and the recommended calculations using a plane strain core.

Comparison of Results -- Figure 1 shows a comparison of the applied stress versus stable crack growth as determined experimentally, as determined using the VR-curve method described in this paper, and as determined using the COA method. The maximum experimental load was approximately 240. MPa (as determined from points in the referenced paper) and the predicted maximum load using the VR-curve method and stress/strain data only was 260.4 MPa, +8%. The maximum calculated load using the COA method was 239. MPa.

The VR-curve method uses a critical crack tip opening displacement criterial for modeling stable crack growth. At the stable crack growth increments, the COA was determined by considering the displacement approximately 1mm behind the crack tip. (Since the mesh was uneven and not coincident with 1mm increments, the nearest grid point to 1mm was used). Figure 2 shows the calculated crack opening angle for successive crack growth increments. The shape of the curve is similar to the experimental curve, but the calculated critical angle at higher stable crack growth increments was in the 4-5 degree range. Because the displaced shape was nonlinear, the COA calculation was strongly dependent on the distance from the crack tip where the calculation was made.

The shapes of the free crack surface were compared using the VR-curve method and the COA method. Results for applied displacements 0.4589 mm and 0.5848 mm are shown in Figures 3 and 4 respectively. Prior to crack initiation and for small crack growth increments, the shape of the free crack surfaces was similar. Note that at the original crack tip location, 12.7 mm, there is a discontinuity in the slope of the displaced shape. For the COA method, this discontinuity is more pronounced. This change in slope results from the permanent plastic strain at the original crack tip. The results for two different meshes were compared for the COA method and are also shown in the figures. For each of the three methods, the predicted stable crack growth increments differed at a given applied load. For the VR-curve method, the shaded region indicates the damage zone where cohesive forces are acting. As the load became larger, differences in the displaced shapes increased.

Description of 2nd Example -- Results were also compared for a

MIDDLE CRACKED ALUMINUM PANEL: $2A/W=.33$

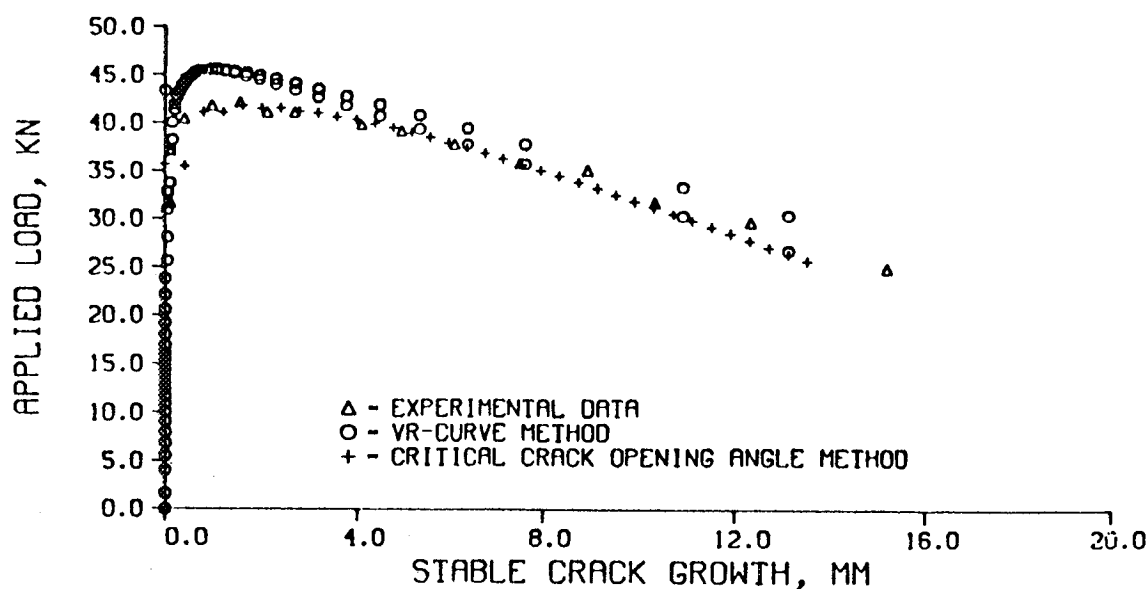


Figure 1: Results for Middle-Cracked Panel

MIDDLE CRACKED ALUMINUM PANEL: $2A/W=.33$

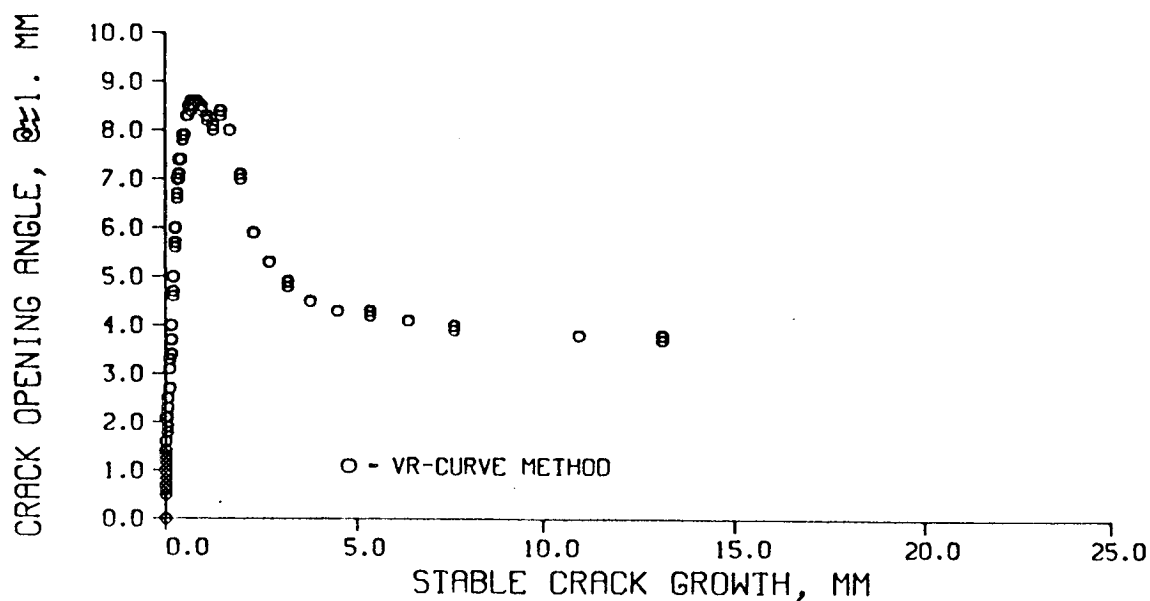


Figure 2: Crack Opening Angle, Middle-Cracked Panel

DISPLACEMENTS ALONG CRACK, YDISP=.4589MM

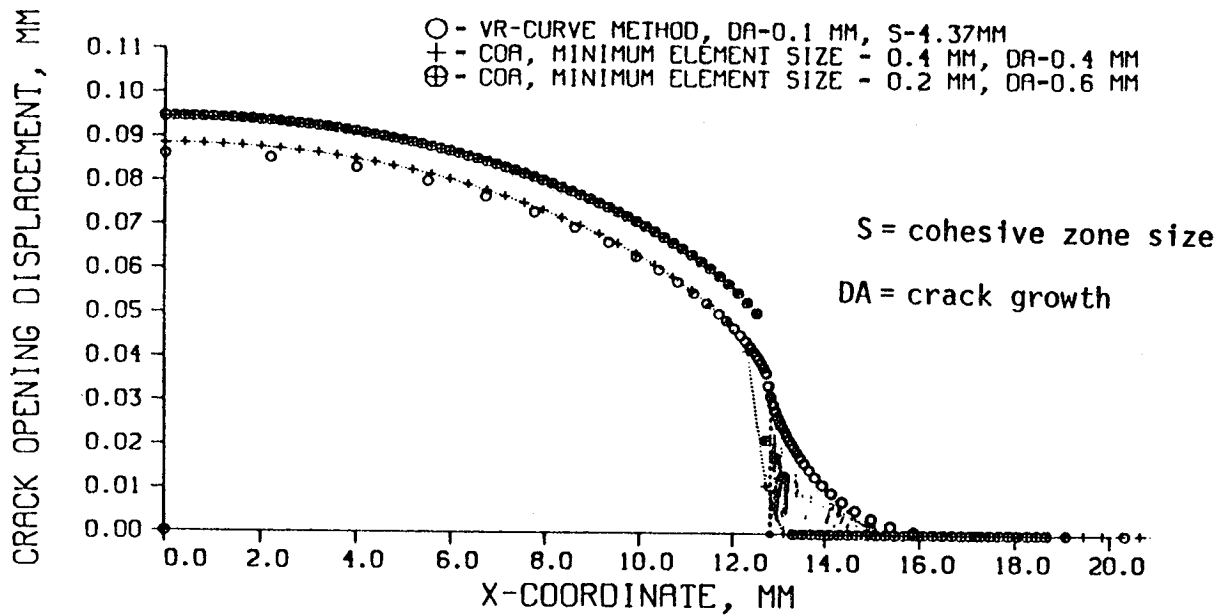


Figure 3: Displacements Along Crack, Middle-Cracked Panel

DISPLACEMENTS ALONG CRACK, YDISP=.5848MM

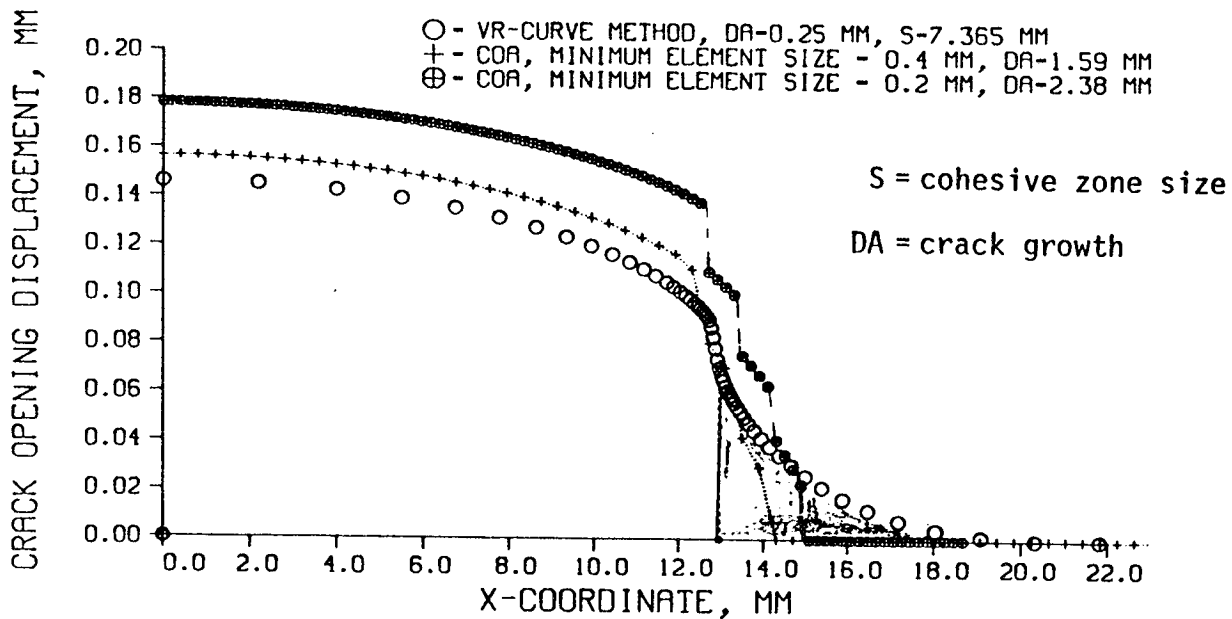


Figure 4: Displacements Along Crack, Middle-Cracked Panel

compact tension specimen fabricated from the same material as Example 1. The geometry of the specimen was described in reference [10] and Figure 5. The applied load versus crack growth behavior is shown in Figure 6. In the experiment, the maximum load of 10.25 kN occurred at 10. mm of crack growth approximately. The VR-curve method predicted a maximum applied load of 10.45 kN at 12.34 mm of stable crack growth. Crack surface displacements before crack initiation and for small increments of crack growth are shown in Figures 7 and 8.

B) Brittle-fracture Example -- For the purposes of analysis, brittle fracture was considered a special case of elastic/plastic fracture. In this example, a compact-tension specimen under plane-strain conditions was evaluated (Figure 9). The load versus crack mouth opening displacement was compared to experimental results [29] and the results are shown in Figure 10. The maximum experimental load was 102.1 kN and the maximum predicted load was 104.0 kN (+1.86%). Since the maximum load differed by 1.86% from the experimental load, the KIC value as calculated according to the ASTM specification [5] also differs by 1.86%.

C) Fatigue Examples

Fatigue Crack Initiation Example -- Fatigue examples were used to predict the number of cycles for crack initiation and to predict the stress versus number of cycles curve. The notched steel bar in Figure 11 was used to predict the number of cycles for crack initiation. For the purposes of this analytic method, an assumed initial crack length is required for analysis. Initial crack lengths of .28 mm (.011") and .33 mm (.013") were chosen to be consistent with experimental measurements when the reference was published [30]. Results for notch depths of .381 mm (.15") and 1.27 mm (.05") are shown in Figure 12.

Fatigue Crack Propagation Example -- The double-notched specimen shown in Figure 13 was used to compare the rate of crack growth to experimental values [31]. Two initial notch lengths were investigated. At the lower applied loads, a very fine mesh is required to capture the dissipative energy effects and correctly model the compressive yield zone. As shown in Figure 14, results at the higher load levels are closer to experimental values. Divergence in results at higher load levels is due in part to mesh size; the same mesh was used for all examples but the size of the compressive yield zone was considerably smaller for the higher load levels.

Discussion and Future Research

Elastic/Plastic and Brittle Fracture Analysis -- Although the elastic/plastic method can be implemented using a general-purpose finite element package, special purpose software would be quicker and easier to use.

Several validation examples for aluminum and steel have been completed. The confidence level for the elastic/plastic method would be enhanced by successful completion of additional examples for a

ELASTIC/PLASTIC FRACTURE, EXAMPLE 2

Material: 2024-T3 Aluminum
Yield Stress: $S_y = 345$ MPa
Ultimate Stress: $S_{ult} = 490$ MPa
Compact-Tension
Thickness = 2.3 mm
Panel width = 190.5 mm
 $a = 61$ mm

Reference: Newman, J.C., Jr., Dawicke, D.S., Sutton, M.A., and Bigelow, C.A., "A Fracture Criterion for Widespread Cracking in Thin-Sheet Aluminum Alloys", International Committee on Aeronautical Fatigue, 17 Symposium, Stockholm, Sweden, 1993.

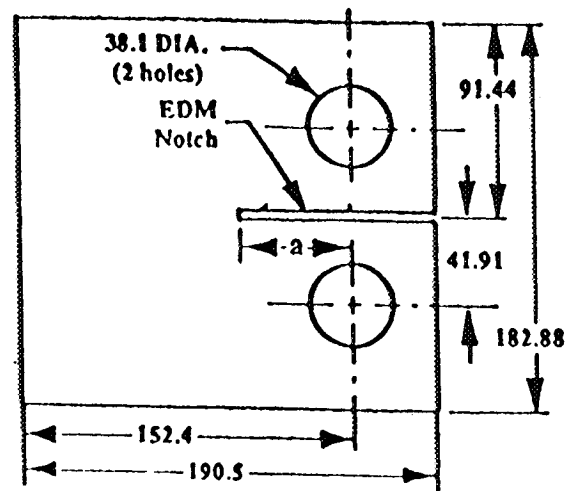


Figure 5: Compact Tension Specimen

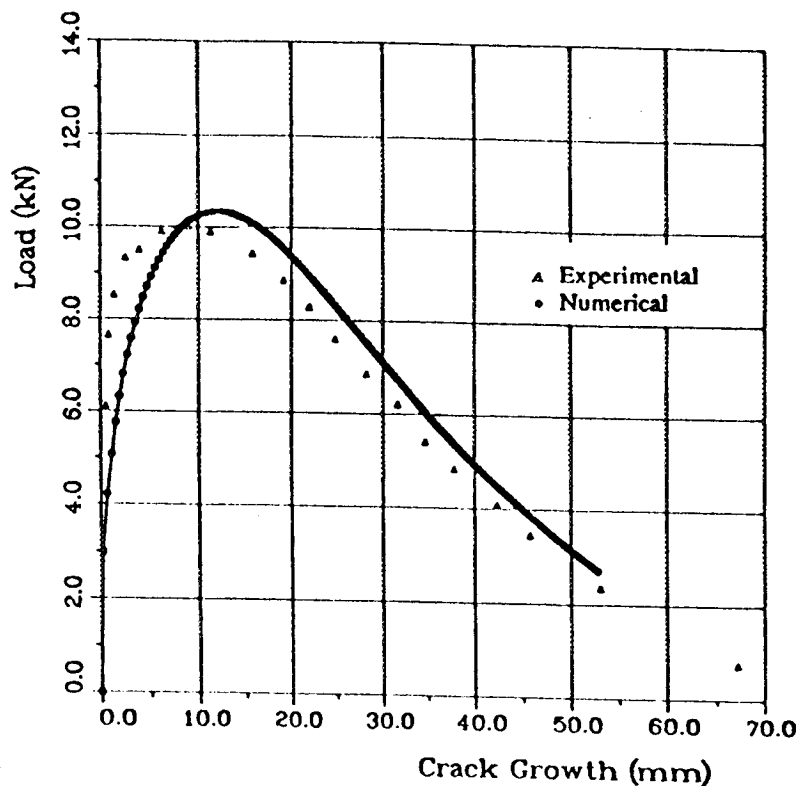


Figure 6: Results, Compact Tension Specimen

COMPACT TENSION SPECIMEN, YDISP=.214 MM

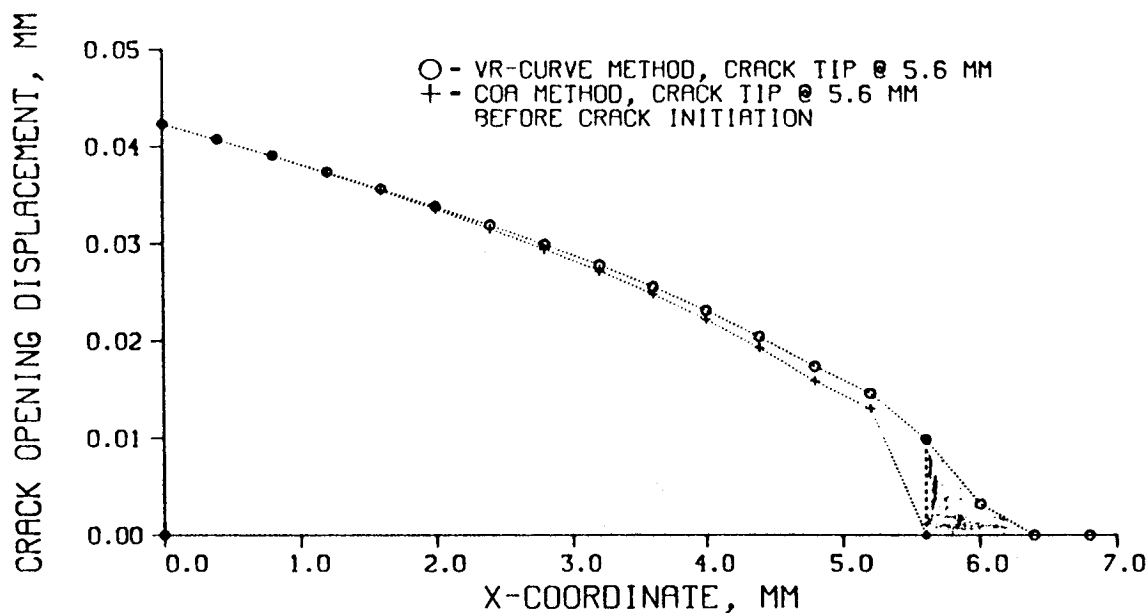


Figure 7: Displacements Along Crack, Compact-Tension Panel (Before Crack Initiation)

COMPACT TENSION SPECIMEN, YDISP=.6852 MM

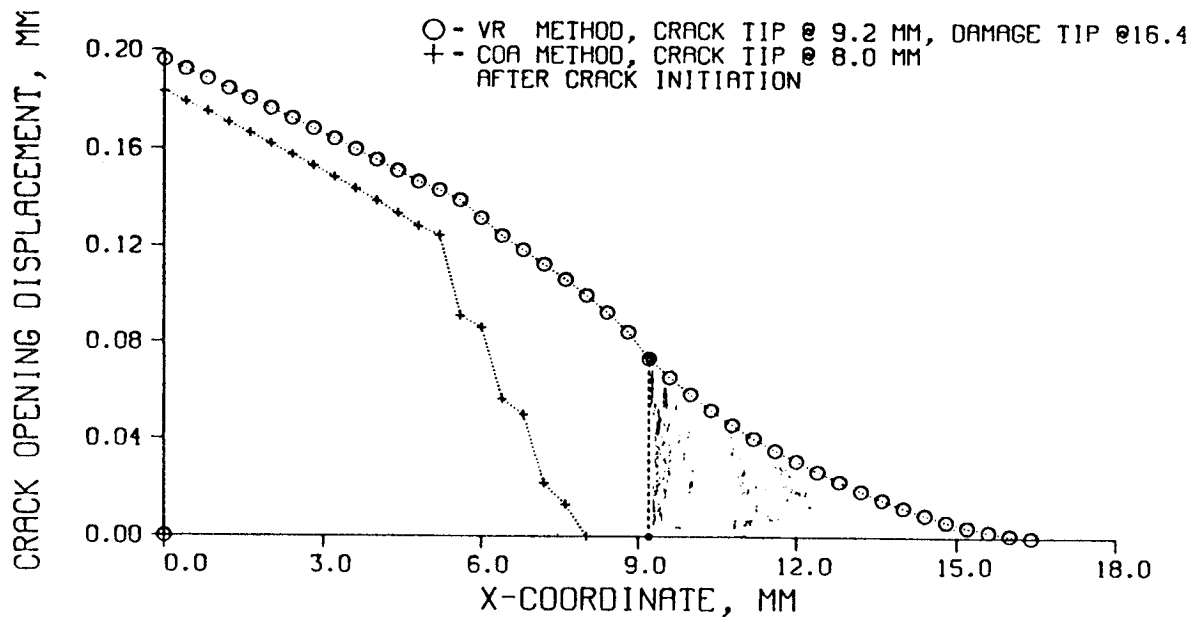


Figure 8: Displacements Along Crack, Compact-Tension Panel (After Crack Initiation)

PLANE STRAIN FRACTURE EXAMPLE

Material: 18Ni Air-Melt Maraging Steel

Yield stress: 190 ksi

Ultimate stress: 196 ksi

Compact tension specimen:

thickness $B = 1.24$ in.

initial crack length $a = 1.95$ in.

width $W = 3.5$ in.

Reference: J.M. Barsom & S.T. Rolfe

Fracture and Fatigue Control in Structures

2nd edition Prentice-Hall, page 89

Figure 9: Brittle Fracture Specimen

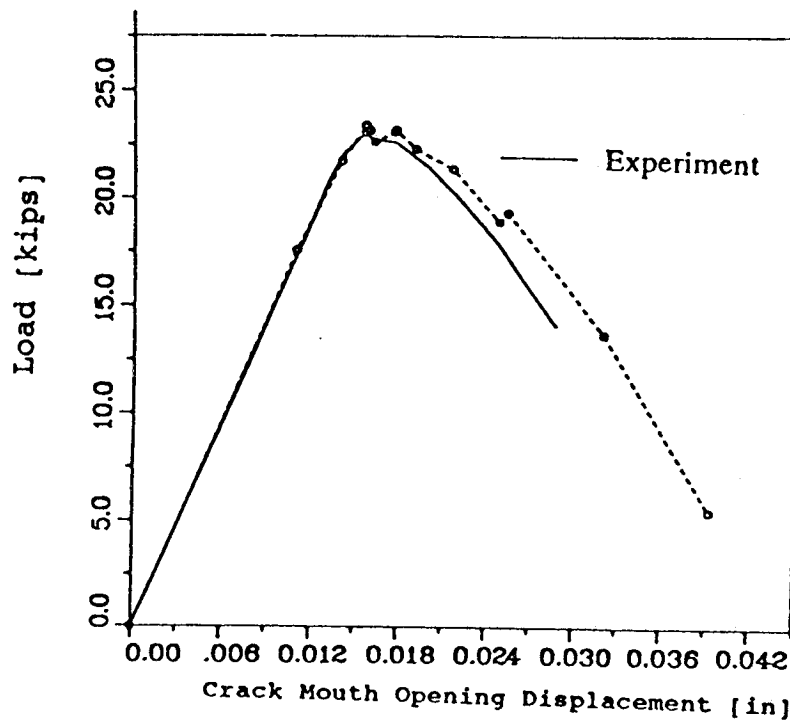
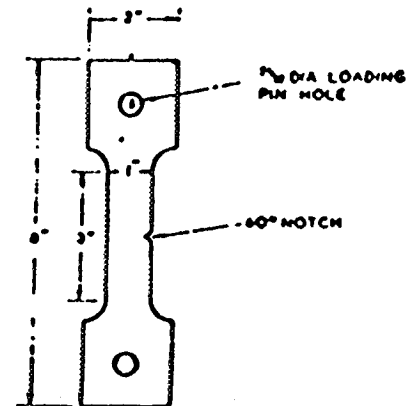


Figure 10: Results, Brittle Fracture

FATIGUE VALIDATION EXAMPLE I

Material: Mild Steel
Yield Stress: 34,720 psi
Ultimate Stress: 60,928 psi
Thickness: 0.2 in.
Notch root radius: 0.002"
Two notch depths studied: 0.05" and 0.15"



Reference: A.R.Jack & A.T.Price, *International Journal of Fracture Mechanics*, Vol. 6, No. 4, December 1970

Figure 11: Side Notch Panel

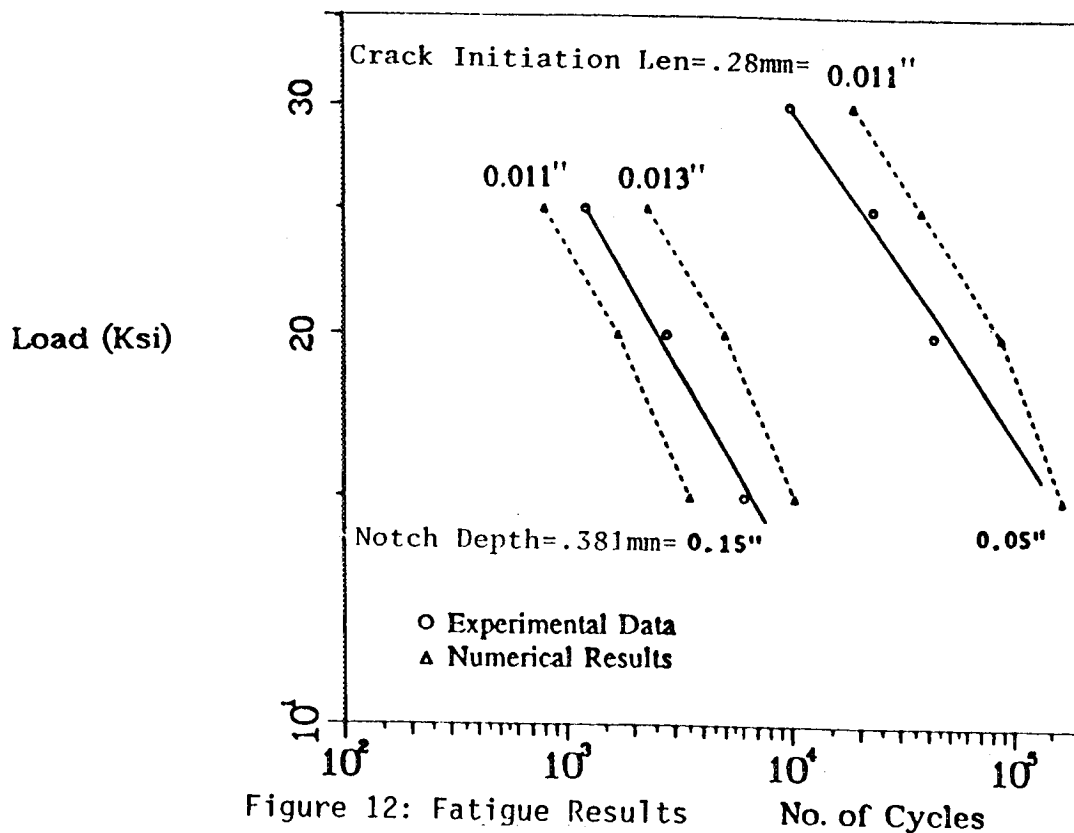
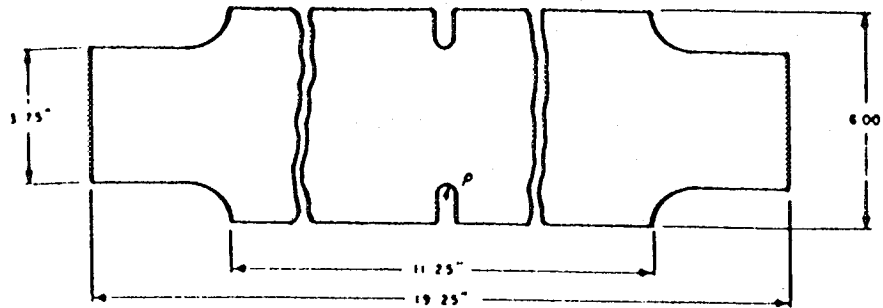


Figure 12: Fatigue Results

(Original figures unavailable at time of publication)

FATIGUE VALIDATION EXAMPLE II



Material: HY130
Yield stress: 146 ksi
Ultimate stress: 153 ksi
Thickness: 0.125"
Two cases studied: root radius 0.016" and 0.064"

Figure 13: Double-Notched Panel

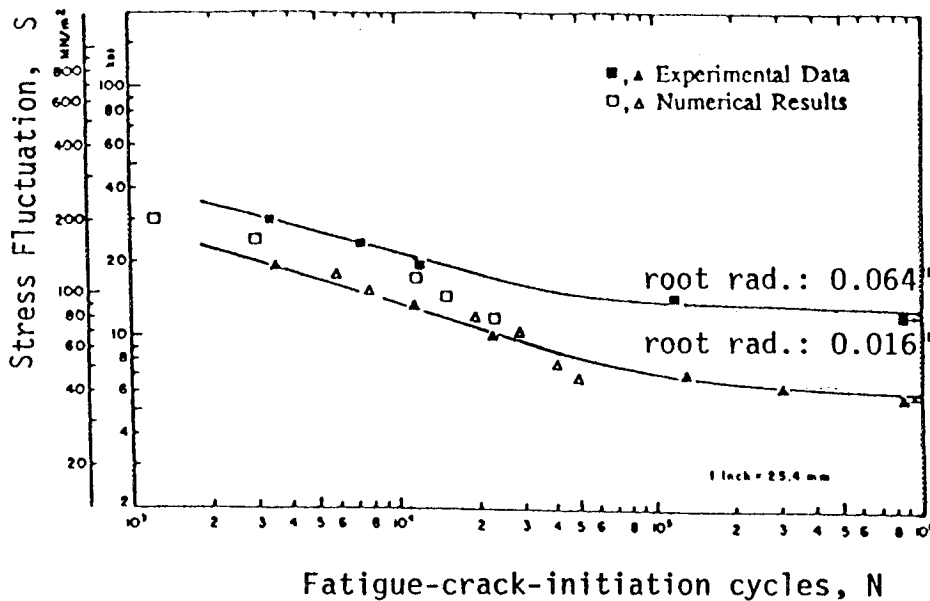


Figure 14: Results, Fatigue Crack Initiation Example
(Double-Notched Panel)

range of metallic alloy materials and geometric shapes. In particular, funding of 'blind' tests for new materials would provide an inexpensive means of increasing the confidence for the method in the engineering community. Similar blind tests would increase the confidence level for predicting KIC.

Fatigue Analysis -- Preliminary results of the fatigue analysis method have been successful. With further development, a special-purpose finite element package could be developed that:

- can be used for either a cracked or flawed specimen
- can predict elastic/plastic crack growth and yield failure
- can predict the critical crack length
- can predict the cycles until crack initiation
- can predict the number of cycles for crack propagation to critical crack length

The package would be applicable to a wide range of geometries and would be designed for use in a range of industries including the automotive, aerospace, and plastics design industries. The package would be written in modular form for expansion into analysis of multi-site damage, creep-fracture, creep-fatigue, and composite materials analysis. Existing special-purpose software such as the programs CRACK IV, FATIGUE and FAST require at least two fatigue constants [32] which would not be required for the proposed software.

Fatigue Crack Initiation -- The research to date indicates that the driving mechanism for fatigue crack growth may be associated with the hysteresis in the stress/strain diagram and the compressive yield zone. The proposed method incorporates this phenomena by use of the E parameter. Additional studies are required to investigate the theoretical basis of this assumption and to determine the optimal means of incorporating this parameter into the fatigue analysis.

Multi-Site Damage -- Unlike most fracture methods which are based on local crack tip damage, the energy parameters used in this analysis method are based on the available and dissipated energy in the structure. The fatigue method is based on two energy parameters W and E. When multiple damage sites are present, the critical crack tip opening displacement curve, generated during the analysis, will be lowered due to the softening effects of multi-site damage and possible crack growth. This softening effect is reflected in the W parameter. Interaction of high stress regions is also captured in the finite element analysis procedure.

The fatigue energy parameter E can also include the effects of multi-site damage. The E parameter sums the energy dissipated at all damage zone nodes experiencing plastic 'shake down' or compressive yield. In the case of multi-site damage, dissipated energy at all damage sites reduces the number of predicted cycles until failure.

Creep-Fatigue -- Presently, predictions of creep fatigue require a material creep law and a series of fatigue constants, each evaluated at a specific state of material creep. Extensive experimental data is

required to determine the C and n constants as a function of the time-dependent creep behavior. The energy-based method proposed in this paper relies on energy assumptions and stress strain diagrams. Material creep law would be required for analysis but fatigue constants would not be required. Nonlinear interactions resulting from cyclic loading under increasing strain due to creep would be incorporated in the critical crack tip opening displacements which are calculated as part of the analysis. A nonlinear creep-fracture method has already been developed by Chang and Kim [33].

Corrosion Fatigue -- Corrosion fatigue cracks have been noted on cargo planes in skin sections with reinforcement straps [34]. The skin section thicknesses are typically within the plane stress region. This type of geometry, thin panels with reinforcing straps, would provide a simple geometry for initial validation of a corrosion fatigue methodology. Corrosion degradation would be incorporated within the material model and corrosion-fatigue constants would not be required.

Composites -- Use of composites in aircraft has increased steadily since the early 1960's. Aircraft such as the F/A 18, the AV 8B, and the V-22 are composed of approximately 10%, 26% and 45% composite materials respectively [35]. Composite materials can result in significant weight savings and an increased resistance to fracture and fatigue. For instance, metal matrix composites with aluminum or titanium matrices have high damage tolerance. Ceramic matrix composites have higher resistance to fracture than unreinforced ceramics while retaining some of the superior high-temperature strength properties.

Existing fracture and fatigue methods are sometimes inappropriate for composite materials due to the lack of standardized ASTM test procedures, the wide variation in material properties, and the likelihood of non-self-similar crack growth. Efforts to evaluate fracture in metal matrix composites and non-self-similar crack growth in glass/epoxy have been initiated [36]. Previous efforts by the authors in predicting Mode II [37] and mixed mode fracture [38] will be helpful for the non-self-similar crack growth problem.

Conclusion

Design engineers typically use finite element methods to check for failure due to buckling and yielding. The method described in this paper uses finite element analysis to predict fracture and fatigue behavior of structures. Once fully developed, the fracture and fatigue methods could find widespread application in aircraft design, engine analysis, bridge design and redesign, and plastics design. The overall safety of fracture-critical designs would be improved without the need for extensive experimental input data.

References

- [1] "F-16 Airframe Structural Integrity Program," from Proceedings of the 1991 USAF Structural Integrity Program Conference, edited by T.D. Cooper, J.W. Lincoln, and R.M. Bader, Wright Patterson Laboratory Report, 1992.
- [2] Landes, H.D., McCabe, D.E., and Ernst, H.A. "Geometry Effects on R-Curve," Nonlinear Fracture Mechanics: Vol II-Elastic-Plastic Fracture, ASTM STP 995, H.D. Landes, A. Saxena, and J.G. Merkle, Eds., American Society for Testing and Materials, Philadelphia, pp. 123-143, 1989.
- [3] Tai, W.H., "An Improvement of CTOD Criterion for Ductile Fracture," Engineering Fracture Mechanics, Vol. 41, pp. 155-157, 1992.
- [4] Kolednik, O., "Loading Conditions May Influence the Shape of J-Da Curves," Engineering Fracture Mechanics, Vol. 41, pp. 251-255, 1992.
- [5] "Standard Method of Test for Plane-strain Fracture Toughness of Metallic Materials," ASTM Designation E-399-83, Vol. 03.01, ASTM Annual Standards, American Society for Testing and Materials, 1985.
- [6] "Standard Practice for R-Curve Determination," ASTM Designation E-561-81, Vol. 03.01, ASTM Annual Standards, American Society for Testing and Materials, 1985.
- [7] "Methods for Crack-tip Opening Displacement (CTOD) Testing," British Standards Institution, BS 5762, 1979.
- [8] Shan, G.X., Kolednik, O., Fischer, F.D., and Stuwe, H.P., "A 2D Model for Numerical Investigations of Stable Crack Growth in Thick Smooth Fracture Mechanics Specimens," Engineering Fracture Mechanics, Vol. 45, pp. 99-106, 1993.
- [9] Elangovan, P.T., "Formulations for Fracture Stress, CTP Zone, and R-Curves," Engineering Fracture Mechanics, Vol. 40, pp. 433-463, 1991.
- [10] Newman, J.C., Jr., Dawicke, D.S., Sutton, M.A., and Bigelow, C.A., "A Fracture Criterion for Widespread Cracking in Thin-Sheet Aluminum Alloys," International Committee on Aeronautical Fatigue, 17 Symposium, Stockholm, Sweden, June 9-11, 1993.
- [11] Zhang, C.H., Gross, D., "Ductile Crack Analysis by a Cohesive Damage Zone Model", Engineering Fracture Mechanics, Vol. 47, pp. 237-248, 1994.
- [12] Paris, P.C., and Erdogan, F., "A Critical Analysis of Crack Propagation Laws, Transactions of the ASME, Journal of Basic Engineering, Series D, Vol. 85, 1963.
- [13] Klesnil, M., and Lukas, P., "Influence of Strength and Stress History on Growth and Stabilization of Fatigue Cracks," Engineering Fracture Mechanics, Vol. 4, pp. 77-92, 1972.

- [14] Mazumdar, P.K., "A Model for High Cycle Fatigue," Engineering Fracture Mechanics, Vol. 21, pp. 907-917, 1992.
- [15] Elber, W., "Fatigue Crack Closure Under Cyclic Tension," Engineering Fracture Mechanics, Vol. 2, pp. 27-45, 1970.
- [16] de Koning, A.U., and Liefthijng, G., "Analysis of Crack Opening Behavior by Application of a Discretized Strip Yield Model," Mechanics of Fatigue Crack Closure, ASTM STP 982, J.C. Newman, Jr. and W. Elber, Eds., American Society for Testing and Materials, Philadelphia, pp. 437-458, 1988.
- [17] Keyvanfar, F., and Nelson, D.V., "Predictions of Fatigue Crack Growth Behavior Using a Crack Closure Ligament Model," Mechanics of Fatigue Crack Closure, ASTM STP 982, J.C. Newman, JR. and W. Elber, EDS., American Society for Testing and Materials, Philadelphia, pp. 437-458, 1988.
- [19] Dawicke, D.S., Grandt, A.F. Jr., and Newman, J.C. Jr., "Three-dimensional Crack Closure Behavior," Engineering Fracture Mechanics, Vol. 36, No. 1, pp., 111-121., 1990.
- [20] Kumar, R., "Review on Crack Closure for Constant Amplitude Loading in Fatigue," Engineering Fracture Mechanics, Vol. 42, pp. 389-400, 1992.
- [21] Dowling, N.E., and Begley, J.A., "Fatigue Crack Growth During Gross Plasticity and the J Integral," ASTM STP 590, American Society for Testing and Materials, Philadelphia, pp. 82-103, 1976.
- [22] Newman Jr., J.C. "A Crack-closure Model for Predicting Fatigue Crack Growth Under Aircraft Spectrum Loading," Methods and Models for Predicting Fatigue Crack Growth under Random Loading, ASTM STP 748, J.B. Chang and C.M. Hudson, Eds., American Society for Testing and Materials, pp. 53-84, 1981.
- [23] Newman Jr., J.C. "Prediction of Fatigue Crack Growth Under Variable-Amplitude and Spectrum Loading Using a Closure Model," Design of Fatigue and Fracture Resistant Structures, ASTM STP 761, P.R. Abelkis and C.M. Hudson, Eds. ASTM, pp. 255-277, 1982.
- [24] Drew, M.W., and Thompson, K.R.L., "The Effect of Overload Cycles on Fatigue Crack Propagation in Two Structural Steels," Engineering Fracture Mechanics, Vol. 30, pp. 579-593, 1988.
- [25] Dexter, R.J., Hudak Jr., S.J., Davidson, D.L., "Modelling and Measurement of Crack Closure and Crack Growth Following Overloads and Underloads," Engineering Fracture Mechanics, Vol. 33, NO. 6, pp. 855-870, 1989.
- [26] Cordes, J., Chang, A., Nelson, N., and Kim, Y., "A Computational Method to Predict Elastic/Plastic Fracture," submitted for review and publication, 11/93.

- [27] Chang, A., Nelson, N., Cordes, J., and Kim, Y., "Fatigue Prediction Based on Computational Fracture Mechanics," accepted for presentation, Third Symposium on Advances in Fatigue Lifetime Predictive Techniques, American Society for Testing and Materials, May, 1994.
- [28] ABAQUS, Hibbitt, Karlsson, Sorensen, Inc., Providence, R.I.
- [29] Barsom, J.M., and Rolfe, S.T., Fracture and Fatigue Control in Structures, 2nd. Edition, Prentice-Hall, Inc., Englewood Cliffs, New Jersey, 1987.
- [30] Jack, A.R., and Price, A.T., "The Initiation of Fatigue Cracks from Notches in Mild Steel Plates," International Journal of Fracture Mechanics, Vol. 6, pp. 401-409, 1970.
- [31] Barsom, J.M., and McNicol, R.C., "Effect of Stress Concentration on Fatigue Crack Initiation in HY-130 Steel," ASTM STP 599, pp. 183-204, 1974.
- [32] Akyurek, T., "A Survey of Fatigue Crack Growth Life Estimation Methodologies," Engineering Fracture Mechanics, Vol. 42, pp. 797-803, 1992.
- [33] Chang, A., and Kim, Y., "Creep Fracture by Finite Element Method," Presented at Joint FEEG/ICF International Conference on Fracture of Engineering Materials and Structures, Singapore, 1991.
- [34] Dunn, W., Shaw, L., and Rogers, L., "Vibroacoustic Fatigue and Stress Corrosion Cracks in the Fuselage Skin of a Large Cargo Airplane," from Proceedings of the 1991 USAF Structural Integrity Program Conference, edited by T.D. Cooper, J.W. Lincoln, and R.M. Bader, Wright Patterson Laboratory Report, 1992.
- [35] Isom, J.L., "A Guide for the Consideration of Composite Material Impacts on Airframe Costs," NTIS Technical Report, AFIT/GCA/LSQ/91S-3, Air Force Institute of Technology, Wright Patterson Air Force Base, OH, 1991.
- [36] Cordes, J., Chang, A., Nelson, N., Kalinowski, J., "Predicting Crack Growth in Continuous-fiber Composite Materials," to be presented at the 26th National Symposium on Fracture Mechanics, Idaho Falls, June 1994.
- [37] Cordes, J., and Yazici, R., "Elastic-Plastic Mode II Fracture in an Aluminum Beam," accepted for publication, Fracture Mechanics: 24 Symposium, ASTM STP 1207, edited by J.D. Landes and D.E. McCabe, American Society for Materials Testing, Philadelphia, 1994.
- [38] Cordes, J., Yazici, R., Seo, M., "Mixed Mode Fracture in Plastically Deforming Materials," Journal of Pressure Vessel Technology, ASME, pp. 348-352, 1993.